PERGAMON

International Journal of Solids and Structures 40 (2003) 89–103

INTERNATIONAL JOURNAL OF SOLIDS and STRUCTURES

www.elsevier.com/locate/ijsolstr

The stress intensity factor history for an advancing crack in a transversely isotropic solid under 3-D loading

Xiaohua Zhao

Department of Civil Engineering, Shantou University, Shantou 515063, China

Received 16 January 2002; received in revised form 8 August 2002

Abstract

The mode I extension of a half plane crack in a transversely isotropic solid under 3-D loading is analyzed. Firstly, the fundamental problem that the crack is subjected to a pair of unit point loads on its faces is considered. Transform methods are used to reduce the boundary value problem to a single integral equation that can be solved by the Wiener–Hopf technique. The Cagniard–de Hoop method is employed to invert the transforms. An exact expression is derived for the mode I stress intensity factor as a function of time and position along the crack edge. Based on the fundamental solution, the stress intensity factor history due to general loading is then obtained. Some features of the solutions are discussed through numerical results.

Keywords: Three-dimensional crack; Transverse isotropy; Transient extension; Stress intensity factor

1. Introduction

With the wide usage of macroscopically anisotropic construction materials such as geomaterials, crystals, and fiber-reinforced composites, elastodynamic analysis of crack problems in such materials has been a subject of considerable interest. The study of these problems is of particular importance to linear elastic fracture mechanics to assess the initiation and growth of a developed macro-crack under dynamic loading conditions, and to nondestructive evaluation for detecting and characterizing the damaged state of the materials. Elastodynamic stress intensity factors produced by incident plane time-harmonic elastic waves have been presented by Ohyoshi (1973) and Zhang and Gross (1993) for antiplane cracks in an infinite transversely isotropic material, and by Dhawan (1982a,b) for inplane cracks. Diffraction of time-harmonic SH waves by an oblique crack in an orthotropic half plane has been investigated by Lobanov and Novichkov (1981), while the diffraction of time-harmonic longitudinal and transverse waves by a semi-infinite crack in an infinite transversely isotropic material has been studied by Norris and Achenbach (1984). Studies for a periodic array of cracks in transversely isotropic solids have been presented by Zhang (1992) for incident SH waves, and by Mandal and Ghosh (1994) for incident P waves. Transient elastodynamic analysis of cracks

E-mail address: xhzhao@stu.edu.cn (X. Zhao).

0020-7683/02/$ - see front matter © 2002 Elsevier Science Ltd. All rights reserved.
PII: S0020-7683(02)00543-7

has been given by Kassir and Bandyopadhyay (1983) and Ang (1987) for an orthotropic solid, and by Shindo et al. (1986, 1992) for an orthotropic strip. The dynamic stress intensity factors have been derived by Ang (1988) for a crack in a layered transversely isotropic material under the action of impact loading, and by Kuo (1984a,b) for an interface crack between orthotropic and fully anisotropic half planes.

All of the above-mentioned references discuss two-dimensional crack problems. But perhaps, because of mathematical complexity, three-dimensional crack problems of an anisotropic material under dynamic loading have not yet received much attention. The interaction of time-harmonic elastic waves with a penny-shaped crack has been analyzed by Tsai (1982, 1988) who calculated the elastodynamic stress intensity factors, and by Kundu and Bostrom (1991, 1992) who computed both the scattered far-field and crack opening displacement (COD). The three-dimensional analysis of cracks in a layered transversely isotropic media has been treated by Lin and Keer (1989). The ultrasonic crack detection in anisotropic materials has been investigated by Mattsson et al. (1997). Exact solutions for a half plane crack in a transversely isotropic material due to both impact loads and moving loads have been obtained by Zhao and Xie (1999, 2000) and Zhao (2000, 2001).

In the present paper, the mode I extension of a half plane crack in a transversely isotropic solid under 3-D loading is analyzed. Aside from being of importance in the field of dynamic fracture mechanics (Freund, 1990), this problem is of practical interest for earthquake engineering. Since the layered rock with faults is usually approximated by a cracked transversely isotropic and linearly elastic solid, the problem can be used to model the initiation of an earthquake. In the analysis, the crack is assumed to propagate with a straight edge. For engineering applications, this solution may be applied to any case where the crack edge curvature is large during extension. In order to obtain the solution of general loading, the solution procedure is divided into two steps. Firstly, the fundamental problem that the crack is subjected to a pair of unit point loads on its faces is considered. Transform methods are used to reduce the boundary value problem to a single integral equation that can be solved by the Wiener–Hopf technique. The Cagniard–de Hoop method is employed to invert the transforms. An exact expression is derived for the mode I stress intensity factor as a function of time and position along the crack edge. Then, the stress intensity factor history due to general loading is obtained using the fundamental solution and the method developed by Freund (1990) for the mode I plane problem. Some features of the solutions are discussed through numerical results.

2. The fundamental solution

2.1. Basic formulas

Consider a transversely isotropic, linear elastic solid containing a half plane crack depicted in Fig. 1. The solid is initially stress free and at rest. A right-handed rectangular coordinate system is introduced such that the y-axis coincides with the crack edge, and the half plane crack occupies the area $z = 0$ and $x < 0$. It is assumed that the symmetric axis of the transversely isotropic material is parallel to the z-axis. At time $t = 0$ a pair of unit point loads appear on the crack faces at the point $(0, 0, 0)$, one acting on the upper face of the crack and the other on the lower face. The directions of the forces are opposite and along the inward normals to each face. Immediately, the crack begins to extend in the x-direction with a constant speed v. Here, we only consider the case $0 < v < c_r$, with c_r being the Rayleigh wave speed of the material. For the solution of general loading, the crack is also assumed to propagate with a straight edge.

Let $u_x(x, y, z, t)$, $u_y(x, y, z, t)$ and $u_z(x, y, z, t)$ denote the relevant displacement components in the x-, y- and z-directions respectively. Then the stresses in the solid can be written as

$$\sigma_{xx} = c_1 \frac{\partial u_x}{\partial x} + c_2 \frac{\partial u_y}{\partial y} + c_3 \frac{\partial u_z}{\partial z}, \tag{1a}$$

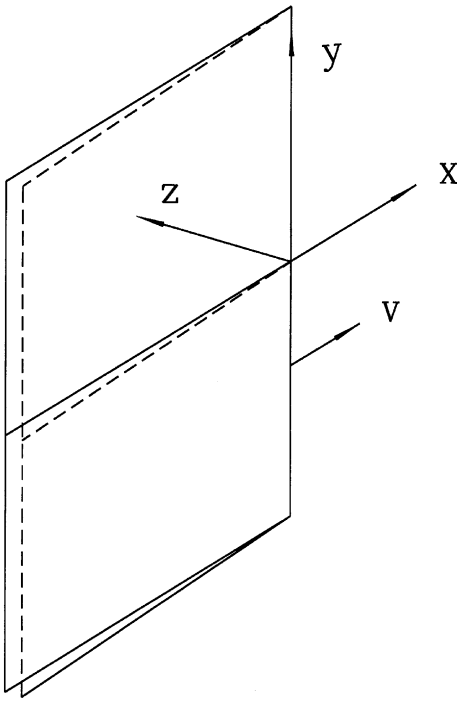

Fig. 1. Geometrical configuration of the elastic solid.

$$\sigma_{yy} = c_2 \frac{\partial u_x}{\partial x} + c_1 \frac{\partial u_y}{\partial y} + c_3 \frac{\partial u_z}{\partial z}, \tag{1b}$$

$$\sigma_{zz} = c_3 \frac{\partial u_x}{\partial x} + c_3 \frac{\partial u_y}{\partial y} + c_4 \frac{\partial u_z}{\partial z}, \tag{1c}$$

$$\sigma_{yz} = c_5 \left[\frac{\partial u_z}{\partial y} + \frac{\partial u_y}{\partial z} \right], \tag{1d}$$

$$\sigma_{xz} = c_5 \left[\frac{\partial u_z}{\partial x} + \frac{\partial u_x}{\partial z} \right], \tag{1e}$$

$$\sigma_{xy} = \frac{1}{2}(c_1 - c_2) \left[\frac{\partial u_x}{\partial y} + \frac{\partial u_y}{\partial x} \right], \tag{1f}$$

where c_k $(k = 1, 2, 3, 4, 5)$ are material constants.

Equations of motion for the problem are expressed by

$$\sigma_{ij,j} = \rho \ddot{\boldsymbol{u}}_i \quad (i = x, y, z), \tag{2}$$

where ρ is the material density.

For a transversely isotropic material it is found to be convenient to introduce scalar potentials $\phi(x, y, z, t)$, $\psi(x, y, z, t)$ and $\theta(x, y, z, t)$, so the displacement components can be represented as

$$u_x = \frac{\partial \phi}{\partial x} + \frac{\partial \psi}{\partial y}, \tag{3a}$$

$$u_y = \frac{\partial \phi}{\partial y} - \frac{\partial \psi}{\partial x}, \tag{3b}$$

$$u_z = \frac{\partial \theta}{\partial z}. \tag{3c}$$

Eliminating the stresses and displacements in Eq. (2), we obtain, after some manipulation, the three equations of motion

$$a_4 \nabla^2 \psi + a_5 \frac{\partial^2 \psi}{\partial z^2} = \frac{\partial^2 \psi}{\partial t^2}, \tag{4a}$$

$$a_3 \nabla^2 \phi + a_5 \nabla^2 \theta + a_2 \frac{\partial^2 \theta}{\partial z^2} = \frac{\partial^2 \theta}{\partial t^2}, \tag{4b}$$

$$a_1 \nabla^2 \phi + a_5 \frac{\partial^2 \phi}{\partial z^2} + a_3 \frac{\partial^2 \theta}{\partial z^2} = \frac{\partial^2 \phi}{\partial t^2}, \tag{4c}$$

where $\nabla^2 = \partial^2/\partial x^2 + \partial^2/\partial y^2$, and the five constants $a_1 = c_1/\rho$, $a_2 = c_4/\rho$, $a_3 = (c_5 + c_3)/\rho$, $a_4 = (c_1 - c_2)/2\rho$, $a_5 = c_5/\rho$.

Using symmetry with respect to the plane $z = 0$, we only consider the region $z \geqslant 0$. The boundary conditions for $z = 0$ are

$$\sigma_{zz}(x, y, 0, t) = -\delta(y)\delta(x)H(t), \quad x < vt, \ -\infty < y < +\infty, \tag{5a}$$

$$\sigma_{xz}(x, y, 0, t) = \sigma_{yz}(x, y, 0, t) = 0, \quad -\infty < x, y < +\infty, \tag{5b}$$

$$u_z(x, y, 0, t) = 0, \quad x \geqslant vt, \ -\infty < y < +\infty. \tag{5c}$$

In the above equations, $H(\cdot)$ is the Heaviside function and $\delta(\cdot)$ is the Dirac delta function.

The initial conditions are expressed in terms of the potentials as

$$\phi(x, y, z, 0) = \psi(x, y, z, 0) = \theta(x, y, z, 0) = 0, \tag{6a}$$

$$\frac{\partial \phi(x, y, z, 0)}{\partial t} = \frac{\partial \psi(x, y, z, 0)}{\partial t} = \frac{\partial \theta(x, y, z, 0)}{\partial t} = 0. \tag{6b}$$

Now we introduce a moving coordinate system (x_1, y, z) by defining

$$x_1 = x - vt, \quad y = y, \quad z = z. \tag{7}$$

In the new coordinate system, Eqs. (4a)–(4c) become

$$a_4 \nabla^2 \psi + a_5 \frac{\partial^2 \psi}{\partial z^2} = \frac{\partial^2 \psi}{\partial t^2} - 2v \frac{\partial^2 \psi}{\partial x_1 \partial t} + v^2 \frac{\partial^2 \psi}{\partial x_1^2}, \tag{8a}$$

$$a_3 \nabla^2 \phi + a_5 \nabla^2 \theta + a_2 \frac{\partial^2 \theta}{\partial z^2} = \frac{\partial^2 \theta}{\partial t^2} - 2v \frac{\partial^2 \theta}{\partial x_1 \partial t} + v^2 \frac{\partial^2 \theta}{\partial x_1^2}, \tag{8b}$$

$$a_1 \nabla^2 \phi + a_5 \frac{\partial^2 \phi}{\partial z^2} + a_3 \frac{\partial^2 \theta}{\partial z^2} = \frac{\partial^2 \phi}{\partial t^2} - 2v \frac{\partial^2 \phi}{\partial x_1 \partial t} + v^2 \frac{\partial^2 \phi}{\partial x_1^2}, \tag{8c}$$

where $\nabla^2 = \partial^2/\partial x_1^2 + \partial^2/\partial y^2$. The boundary conditions for $z = 0$ can be written as

$$\sigma_{zz}(x_1, y, 0, t) = -\delta(y)\delta(x_1 + vt)H(t), \quad x_1 < 0, \ -\infty < y < +\infty, \tag{9a}$$

$$\sigma_{xz}(x_1, y, 0, t) = \sigma_{yz}(x_1, y, 0, t) = 0, \quad -\infty < x_1, y < +\infty, \tag{9b}$$

$$u_z(x_1, y, 0, t) = 0, \quad x_1 \geqslant 0, \ -\infty < y < +\infty. \tag{9c}$$

2.2. The solution procedure

Transform methods and the Wiener–Hopf technique are used to solve this fundamental problem. The first step is to apply a one-sided Laplace transform over time to the partial differential equations (8a)–(8c), taking into account the initial conditions. The transformed function is denoted by a superposed hat, for example,

$$\widehat{\phi}(x_1, y, z, s) = \int_0^\infty \phi(x_1, y, z, t)\mathrm{e}^{-st}\,\mathrm{d}t, \tag{10}$$

where the complex number s has a positive real part. Next, a two-sided Laplace transform is introduced over the y coordinate. The complex transform parameter is $s\xi$, and the transformed function is denoted by a bar, i.e.

$$\overline{\phi}(x_1, \xi, z, s) = \int_{-\infty}^{+\infty} \widehat{\phi}(x_1, y, z, s)\mathrm{e}^{-s\xi y}\,\mathrm{d}y. \tag{11}$$

Finally, a two-sided Laplace transform is used to suppress the dependence on x_1. The complex transform parameter is $s\eta$, and the transformed function is denoted as

$$\phi^*(\eta, \xi, z, s) = \int_{-\infty}^{+\infty} \overline{\phi}(x_1, \xi, z, s)\mathrm{e}^{-s\eta x_1}\,\mathrm{d}x_1. \tag{12}$$

The partial differential equations (8a)–(8c) are reduced to

$$-a_4 s^2 \mu_3^2 \psi^* + a_5 \frac{\mathrm{d}^2\psi^*}{\mathrm{d}z^2} = 0, \tag{13a}$$

$$a_3 s^2(\eta^2 + \xi^2)\phi^* - a_5 s^2 \mu_2^2 \theta^* + a_2 \frac{\mathrm{d}^2\theta^*}{\mathrm{d}z^2} = 0, \tag{13b}$$

$$-a_1 s^2 \mu_1^2 \phi^* + a_5 \frac{\mathrm{d}^2\phi^*}{\mathrm{d}z^2} + a_3 \frac{\mathrm{d}^2\theta^*}{\mathrm{d}z^2} = 0, \tag{13c}$$

where

$$\mu_1(\eta, \xi) = [p_1^2(1 - v\eta)^2 - \eta^2 - \xi^2]^{1/2}, \tag{14}$$

$$\mu_2(\eta, \xi) = [p_2^2(1 - v\eta)^2 - \eta^2 - \xi^2]^{1/2}, \tag{15}$$

$$\mu_3(\eta, \xi) = [p_3^2(1 - v\eta)^2 - \eta^2 - \xi^2]^{1/2}, \tag{16}$$

$$p_1^2 = a_1^{-1}, \quad p_2^2 = a_5^{-1}, \quad p_3^2 = a_4^{-1}. \tag{17}$$

The branch points of $\mu_1(\eta, \xi)$, $\mu_2(\eta, \xi)$ and $\mu_3(\eta, \xi)$ can be obtained by letting

$$\mu_1(\eta, \xi) = 0, \quad \mu_2(\eta, \xi) = 0, \quad \mu_3(\eta, \xi) = 0, \tag{18}$$

which yield

$$\eta_{1,2} = \frac{-p_1^2 v \pm \sqrt{p_1^4 v^2 + (1 - p_1^2 v^2)(p_1^2 - \xi^2)}}{1 - p_1^2 v^2} \quad \text{for } \mu_1(\eta, \xi), \tag{19a}$$

$$\eta_{3,4} = \frac{-p_2^2 v \pm \sqrt{p_2^4 v^2 + (1 - p_2^2 v^2)(p_2^2 - \xi^2)}}{1 - p_2^2 v^2} \quad \text{for } \mu_2(\eta, \xi), \tag{19b}$$

$$\eta_{5,6} = \frac{-p_3^2 v \pm \sqrt{p_3^4 v^2 + (1 - p_3^2 v^2)(p_3^2 - \xi^2)}}{1 - p_3^2 v^2} \quad \text{for } \mu_3(\eta, \xi). \tag{19c}$$

The complex η plane is cut along $-\infty < \mathrm{Re}(\eta) < \eta_2$, $\eta_1 < \mathrm{Re}(\eta) < \infty$, $\mathrm{Im}(\eta) = 0$ so that $\mathrm{Re}(\mu_1) \geqslant 0$ in the entire cut η plane for each value of η, and likewise for $\mathrm{Re}(\mu_2, \mu_3) \geqslant 0$.

The solutions of Eqs. (13a)–(13c), bounded as $z \to \infty$, are

$$\phi^* = A\mathrm{e}^{-s\lambda_1 z} + B\mathrm{e}^{-s\lambda_2 z}, \tag{20a}$$

$$\theta^* = \frac{a_1\mu_1^2 - a_5\lambda_1^2}{a_3\lambda_1^2} A\mathrm{e}^{-s\lambda_1 z} + \frac{a_1\mu_1^2 - a_5\lambda_2^2}{a_3\lambda_2^2} B\mathrm{e}^{-s\lambda_2 z}, \tag{20b}$$

$$\psi^* = C\mathrm{e}^{-s\lambda_3 z}, \tag{20c}$$

where A, B, C are arbitrary functions of ξ and η, and

$$\lambda_{1,2}^2 = \frac{L(\eta^2 + \xi^2) + (a_2 + a_5)(1 - v\eta)^2}{2a_2 a_5} \pm \left\{ \left[\frac{L(\eta^2 + \xi^2) + (a_2 + a_5)(1 - v\eta)^2}{2a_2 a_5} \right]^2 - \frac{a_1}{a_2}\mu_1^2\mu_2^2 \right\}^{1/2}, \tag{21}$$

$$\lambda_3 = \sqrt{\frac{a_4}{a_5}}\mu_3, \tag{22}$$

$$L = a_3^2 - a_5^2 - a_1 a_2. \tag{23}$$

The boundary conditions are now transformed. With reference to Eqs. (9a)–(9c), define two functions $\sigma_+(x_1, y, t)$ and $u_-(x_1, y, t)$ by

$$\sigma_+(x_1, y, t) = \begin{cases} \sigma_{zz}(x_1, y, 0, t), & x_1 \geqslant 0, \\ 0, & x_1 < 0, \end{cases} \tag{24a}$$

$$u_-(x_1, y, t) = \begin{cases} 0, & x_1 \geqslant 0, \\ u_z(x_1, y, 0, t), & x_1 < 0. \end{cases} \tag{24b}$$

The boundary conditions are then transformed to

$$\rho s^2 \left[(a_3 - a_5)(\eta^2 + \xi^2) + \frac{a_2}{a_3}(a_1\mu_1^2 - a_5\lambda_1^2) \right] A + \rho s^2 \left[(a_3 - a_5)(\eta^2 + \xi^2) + \frac{a_2}{a_3}(a_1\mu_1^2 - a_5\lambda_2^2) \right] B = \frac{1}{s}\Sigma_+(\eta, \xi, s) - \frac{1}{s(1 - v\eta)}, \tag{25a}$$

$$\left(\frac{a_1\mu_1^2 - a_5\lambda_1^2}{a_3\lambda_1} + \lambda_1 \right) \xi A + \left(\frac{a_1\mu_1^2 - a_5\lambda_2^2}{a_3\lambda_2} + \lambda_2 \right) \xi B - \eta\lambda_3 C = 0, \tag{25b}$$

$$\left(\frac{a_1\mu_1^2 - a_5\lambda_1^2}{a_3\lambda_1} + \lambda_1\right)\eta A + \left(\frac{a_1\mu_1^2 - a_5\lambda_2^2}{a_3\lambda_2} + \lambda_2\right)\eta B + \xi\lambda_3 C = 0, \tag{25c}$$

$$-s^3\left(\frac{a_1\mu_1^2 - a_5\lambda_1^2}{a_3\lambda_1}A + \frac{a_1\mu_1^2 - a_5\lambda_2^2}{a_3\lambda_2}B\right) = U_-(\eta,\xi,s), \tag{25d}$$

where

$$\Sigma_+(\eta,\xi,s) = s\int_{-\infty}^{+\infty}\int_{-\infty}^{+\infty}\widehat{\sigma}_+(x_1,y,s)\exp[-s(\xi y + \eta x_1)]\,\mathrm{d}y\,\mathrm{d}x_1, \tag{26}$$

$$U_-(\eta,\xi,s) = s^2\int_{-\infty}^{+\infty}\int_{-\infty}^{+\infty}\widehat{u}_-(x_1,y,s)\exp[-s(\xi y + \eta x_1)]\,\mathrm{d}y\,\mathrm{d}x_1. \tag{27}$$

If A, B, C are eliminated from Eqs. (25a)–(25d), the result is a single equation involving the two remaining unknown functions Σ_+ and U_-, namely

$$-\frac{\rho R(\eta,\xi)}{\mu_1(\eta,\xi)}U_- = \frac{1}{v\eta - 1} + \Sigma_+, \tag{28}$$

in which

$$R(\eta,\xi) = \frac{\{[(a_3 - a_5)^2 - a_1a_2](\eta^2 + \xi^2) + a_2(1 - v\eta)^2\}\mu_2 + \sqrt{a_1a_2}\mu_1(1 - v\eta)^2}{\sqrt{a_1a_2}(\lambda_1 + \lambda_2)}. \tag{29}$$

Eq. (28) is of the type that can be solved by the Wiener–Hopf technique, so we may determine Σ_+ and U_- with a single equation. The Wiener–Hopf procedure requires that the mixed functions in (28) must be factored into the product of sectionally analytic functions. To do this, we rewrite $R(\eta,\xi)$ into the following form:

$$\begin{aligned} R(\eta,\xi) = {} & \frac{a_1a_5[a_1a_2 - (a_3 - a_5)^2](\mu_1 + \mu_2)}{4\sqrt{a_1a_2}(a_1 - a_5)(\lambda_1 + \lambda_2)(1 - v\eta)^2}\{4(\eta^2 + \xi^2)\mu_1\mu_2 + (\mu_2^2 - \eta^2 - \xi^2)^2 \\ & + P(1 - v\eta)^2[(\eta^2 + \xi^2) + \mu_1\mu_2] + Q(1 - v\eta)^4\}, \end{aligned} \tag{30}$$

where

$$P = \frac{4(\sqrt{a_1a_2} - a_2)}{a_1a_2 - (a_3 - a_5)^2}, \tag{31}$$

$$Q = \frac{P}{\sqrt{a_1a_2}} + \frac{a_2(a_2 - a_1) + (a_3 + a_5 - a_2)(a_3 + a_2 - 3a_5)}{a_5^2[a_1a_2 - (a_3 - a_5)^2]}. \tag{32}$$

It is proved that $R(\eta,\xi)(1 - v\eta)^{-2} = 0$ has only two roots in the η plane, which can be expressed as

$$c_{1,2} = \frac{-c^2v \pm \sqrt{c^4v^2 + (1 - c^2v^2)(c^2 - \xi^2)}}{1 - c^2v^2}, \tag{33}$$

where $c = c_r^{-1}$.

Introduce a new function by defining

$$S(\eta,\xi) = -\frac{R(\eta,\xi)}{k_1k_2(\eta - c_1)(\eta - c_2)(1 - v\eta)^2}. \tag{34}$$

Then, we have

$$S(\eta,\xi)=S_1(\eta,\xi)S_2(\eta,\xi), \tag{35}$$

where

$$S_1(\eta,\xi)=\frac{a_1a_5}{2(a_5-a_1)k_1} \times\frac{4(\eta^2+\xi^2)\mu_1\mu_2+(\mu_2^2-\eta^2-\xi^2)^2+P(1-v\eta)^2[(\eta^2+\xi^2)+\mu_1\mu_2]+Q(1-v\eta)^4}{(1-v\eta)^4(\eta-c_1)(\eta-c_2)}, \tag{36}$$

$$S_2(\eta,\xi)=\frac{a_1a_2-(a_3-a_5)^2}{2k_2\sqrt{a_1a_2}}\frac{\mu_1+\mu_2}{\lambda_1+\lambda_2}, \tag{37}$$

$$k_1=\frac{a_1a_5k_3}{2(a_5-a_1)v^4}, \tag{38}$$

$$k_2=\sqrt{\frac{a_5}{2a_1}}\frac{[a_1a_2-(a_3-a_5)^2]\left(\sqrt{1-p_1^2v^2}+\sqrt{1-p_2^2v^2}\right)}{\{-\sqrt{k_4}-[L+(a_2+a_5)v^2]\}^{1/2}+\{\sqrt{k_4}-[L+(a_2+a_5)v^2]\}^{1/2}}, \tag{39}$$

$$k_3=-4(1-p_1^2v^2)^{1/2}(1-p_2^2v^2)^{1/2}+(2-p_2^2v^2)^2+Pv^2[1-(1-p_1^2v^2)^{1/2}(1-p_2^2v^2)^{1/2}]+Qv^4, \tag{40}$$

$$k_4=[L+(a_2+a_5)v^2]^2-4a_1a_2a_5^2(1-p_1^2v^2)(1-p_2^2v^2). \tag{41}$$

The function $S_1(\eta,\xi)$ has no poles or zeros in the complex η plane, the only singularities being the branch points of the functions $\mu_1(\eta,\xi)$ and $\mu_2(\eta,\xi)$. In the entire cut η plane, $S_1(\eta,\xi)$ is analytic. When $|\eta|\to\infty$, $S_1(\eta,\xi)\to 1$. According to Cauchy's integral theorem, $S_1(\eta,\xi)$ can be decomposed into

$$S_1(\eta,\xi)=S_1^+(\eta,\xi)S_1^-(\eta,\xi), \tag{42}$$

where

$$S_1^{\pm}(\eta,\xi)=\exp\left\{-\frac{1}{\pi}\int_{p_1}^{p_2} tg^{-1}\left[\frac{(4\varsigma^2+P)\sqrt{p_2^2-\varsigma^2}\sqrt{\varsigma^2-p_1^2}}{(p_2^2-2\varsigma^2)^2+P\varsigma^2+Q}\right]f_{\pm}(\eta,\xi,\varsigma)\,\mathrm{d}\varsigma\right\}, \tag{43}$$

$$f_{\pm}(\eta,\xi,\varsigma)=\frac{\varsigma\left[\pm 2v\sqrt{(1+v^2\xi^2)\varsigma^2-\xi^2}+(1+v^2\xi^2)(1+v^2\varsigma^2)-2v^2\xi^2\right]}{(1-v^2\varsigma^2)\sqrt{(1+v^2\xi^2)\varsigma^2-\xi^2}\left[\pm v\varsigma^2+\sqrt{(1+v^2\xi^2)\varsigma^2-\xi^2}\pm\eta(1-v^2\varsigma^2)\right]}. \tag{44}$$

The functions $S_1^+(\eta,\xi)$ and $S_1^-(\eta,\xi)$ are analytic and nonzero in the regions $\mathrm{Re}(\eta)>\eta_2$ and $\mathrm{Re}(\eta)<\eta_1$, respectively.

The singularities of $S_2(\eta,\xi)$ in the complex η plane are the branch points of the functions $\lambda_1(\eta,\xi)$, $\lambda_2(\eta,\xi)$, $\mu_1(\eta,\xi)$ and $\mu_2(\eta,\xi)$. The functions $\lambda_1(\eta,\xi)$ and $\lambda_2(\eta,\xi)$ possess two kinds of branch points. The first kind of branch points are those given by Eqs. (19a) and (19b), which correspond to $\lambda_1(\eta,\xi)=0$ or $\lambda_2(\eta,\xi)=0$. The second kind of branch points are where $\lambda_2^2(\eta,\xi)-\lambda_1^2(\eta,\xi)$ is zero. Such points will appear in pairs. Between the two points of a given pair we may define a branch cut such that $\lambda_1(\eta,\xi)+\lambda_2(\eta,\xi)$ is continuous across the cut while $\lambda_1(\eta,\xi)$ and $\lambda_2(\eta,\xi)$ are each discontinuous. Therefore, these cuts give no contribution to the analytic factorization. So we obtain via the use of Cauchy's integral theorem

$$S_2(\eta,\xi)=S_2^+(\eta,\xi)S_2^-(\eta,\xi), \tag{45}$$

where

$$S_2^{\pm}(\eta,\xi)=\exp\left\{-\frac{1}{\pi}\int_{p_1}^{p_2} tg^{-1}\left[\frac{\beta_1\sqrt{\varsigma^2-p_1^2}-\beta_2\sqrt{p_2^2-\varsigma^2}}{\beta_1\sqrt{p_2^2-\varsigma^2}+\beta_2\sqrt{\varsigma^2-p_1^2}}\right]f_{\pm}(\eta,\xi,\varsigma)\,\mathrm{d}\varsigma\right\}, \tag{46}$$

$$\beta_{1,2}=\left\{\sqrt{\left[\frac{L\varsigma^2+a_2+a_5}{2a_2a_5}\right]^2+\frac{a_1}{a_2}(\varsigma^2-p_1^2)(p_2^2-\varsigma^2)}\pm\frac{L\varsigma^2+a_2+a_5}{2a_2a_5}\right\}^{1/2}. \tag{47}$$

The functions $S_2^+(\eta,\xi)$ and $S_2^-(\eta,\xi)$ are analytic and nonzero in the regions $\mathrm{Re}(\eta)>\eta_2$ and $\mathrm{Re}(\eta)<\eta_1$, respectively.

Thus we have

$$S(\eta,\xi)=S_+(\eta,\xi)S_-(\eta,\xi) \tag{48}$$

with

$$S_{\pm}(\eta,\xi)=S_1^{\pm}(\eta,\xi)S_2^{\pm}(\eta,\xi). \tag{49}$$

We also have

$$\mu_1(\eta,\xi)=\sqrt{1-p_1^2v^2}\sqrt{\eta-\eta_2}\sqrt{\eta_1-\eta}. \tag{50}$$

Let

$$F_+(\eta,\xi)=\frac{\sqrt{\eta-\eta_2}}{(\eta-c_2)S_+(\eta,\xi)} \tag{51a}$$

and

$$F_-(\eta,\xi)=\frac{\sqrt{\eta_1-\eta}}{(\eta-c_1)S_-(\eta,\xi)}. \tag{51b}$$

Then Eq. (28) becomes

$$\frac{\rho k_1k_2(1-v\eta)^2}{\sqrt{1-p_1^2v^2}F_-(\eta,\xi)}U_-=\frac{1}{v\eta-1}F_+(\eta,\xi)+F_+(\eta,\xi)\Sigma_+. \tag{52}$$

It is noticed that the only singularity of the mixed function in (52) in the right half plane is a simple pole at $\eta=v^{-1}$. This singularity can be removed by requiring the residue to be zero, so we obtain

$$\frac{\rho k_1k_2(1-v\eta)^2}{\sqrt{1-p_1^2v^2}F_-(\eta,\xi)}U_--\frac{1}{v\eta-1}F_+(v^{-1},\xi)=\frac{1}{v\eta-1}[F_+(\eta,\xi)-F_+(v^{-1},\xi)]+F_+(\eta,\xi)\Sigma_+. \tag{53}$$

The right-hand side of Eq. (53) is analytic in the region $\mathrm{Re}(\eta)>\eta_2$, and the left-hand side is analytic in $\mathrm{Re}(\eta)<\min(\eta_1,v^{-1})$. Therefore, by analytic continuation, each side of (53) represents the same entire function $E(\eta,\xi,s)$. According to Liouville's theorem, a bounded entire function is a constant. In this case, $E(\eta,\xi,s)$ is bounded in the finite plane and $E(\eta,\xi,s)\to 0$ as $|\eta|\to\infty$. Thus $E(\eta,\xi,s)\equiv 0$, and we obtain

$$\Sigma_+=\frac{1}{v\eta-1}\left[\frac{F_+(v^{-1},\xi)}{F_+(\eta,\xi)}-1\right], \tag{54}$$

$$U_-=\frac{\sqrt{1-p_1^2v^2}}{\rho k_1k_2(v\eta-1)^3}F_+(v^{-1},\xi)F_-(\eta,\xi). \tag{55}$$

2.3. The dynamic stress intensity factor

When the normal stress on the crack plane $z = 0$ has been obtained, we come to the determination of the dynamic stress intensity factor for the fundamental problem. The stress intensity factor in the Laplace transform dormain can be expressed as

$$\bar{k}_{\mathrm{I}}^{\mathrm{F}}(\xi, s) = \lim_{x_1 \to 0^+} [(2\pi x_1)^{1/2} \bar{\sigma}_+(x_1, \xi, s)]. \tag{56}$$

From the Abel theorem concerning asymptotic properties of transforms and by virtue of Eqs. (26) and (54), we obtain

$$\bar{k}_{\mathrm{I}}^{\mathrm{F}}(\xi, s) = \lim_{\eta \to \infty} [(2s\eta)^{1/2} \Sigma_+ \cdot s^{-1}] = \frac{\sqrt{2}}{s^{1/2} v} F_+(v^{-1}, \xi). \tag{57}$$

Further, we have

$$\bar{k}_{\mathrm{I}}^{\mathrm{F}}(\xi, s) = \frac{\sqrt{2}}{s^{1/2} v} \frac{\sqrt{v^{-1} - \eta_2}}{(v^{-1} - c_2) S_+(v^{-1}, \xi)}. \tag{58}$$

The inverse two-sided Laplace transform of (58) is

$$\overset{\frown}{k}_{\mathrm{I}}^{\mathrm{F}}(y, s) = \frac{s}{2\pi \mathrm{i}} \int_{\alpha_0 - \mathrm{i}\infty}^{\alpha_0 + \mathrm{i}\infty} \frac{\sqrt{2}}{s^{1/2} v} \frac{\sqrt{v^{-1} - \eta_2}}{(v^{-1} - c_2) S_+(v^{-1}, \xi)} \exp(s\xi y)\, \mathrm{d}\xi, \tag{59}$$

where $y > 0$ is assumed for the time being.

The Cagniard–de Hoop method is used for the inversion. It is easily known that the integrand of (59) has the branch points of $\xi = \pm a_0$, $\xi = \pm b_0$ and $\xi = \pm c_0$ in the ξ plane with

$$a_0 = \sqrt{\frac{p_1^2}{1 - p_1^2 v^2}}, \quad b_0 = \sqrt{\frac{p_2^2}{1 - p_2^2 v^2}}, \quad c_0 = \sqrt{\frac{c^2}{1 - c^2 v^2}}. \tag{60}$$

In order that the final inversion of the one-sided Laplace transform over time may be performed by inspection, we now shift the ξ integration to the contour as shown in Fig. 2. The integrand of (59) is analytic and single-valued inside this contour. According to Cauchy's integral theorem and Jordan's lemma, we have

$$\overset{\frown}{k}_{\mathrm{I}}^{\mathrm{F}}(y, s) = -\frac{\sqrt{2s}(1 - c^2 v^2)}{\pi \sqrt{v(1 - p_1^2 v^2)}} \int_{a_0}^{\infty} \mathrm{Im} \left\{ \frac{\left[1 + v\sqrt{p_1^2 - (1 - p_1^2 v^2)\xi^2}\right]^{1/2}}{\left[1 + v\sqrt{c^2 - (1 - c^2 v^2)\xi^2}\right] S_+(v^{-1}, \xi)} \right\} \exp(-s\xi y)\, \mathrm{d}\xi. \tag{61}$$

Upon noting that $k_{\mathrm{I}}^{\mathrm{F}}(y, t)$ is an even function of y and from the convolution theorem for Laplace transform, we finally obtain

$$k_{\mathrm{I}}^{\mathrm{F}}(y, t) = \frac{\sqrt{2}(c^2 v^2 - 1)}{\pi^{3/2} \sqrt{v(1 - p_1^2 v^2)}} \int_{a_0}^{t/|y|} \frac{\partial}{\partial \xi} \mathrm{Im} \left\{ \frac{\left[1 + v\sqrt{p_1^2 - (1 - p_1^2 v^2)\xi^2}\right]^{1/2}}{\left[1 + v\sqrt{c^2 - (1 - c^2 v^2)\xi^2}\right] S_+(v^{-1}, \xi)} \right\} \frac{\mathrm{d}\xi}{|y| \sqrt{t - |y|\xi}}. \tag{62}$$

3. Case of general loading

We now consider the extension of the half plane crack under general loading. Suppose that the crack is stationary for $t < 0$ under equilibrium loading, and the resulting normal stress in the z-direction along $x > 0$,

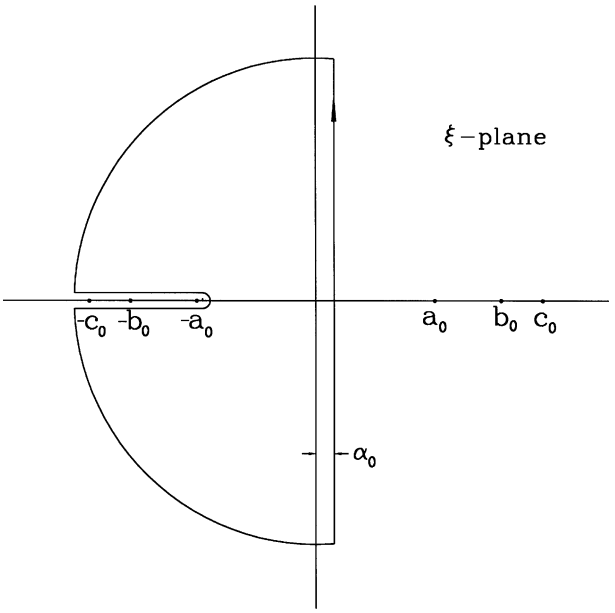

Fig. 2. The integration contour.

$z = 0$ is $\sigma_{zz}(x, y, 0) = p(x, y)$. At time $t = 0$, the crack begins to extend in the x-direction with a constant speed v, creating new traction-free surfaces ($0 < x < vt,\ -\infty < y < \infty,\ z = \pm 0$). The stress wave field associated with the extension may be considered to be the superposition of the dynamic field created by imposing tractions $-p(x, y)$ ($0 < x < vt,\ -\infty < y < \infty,\ z = \pm 0$) on the crack faces, and the static field for $t < 0$.

The dynamic field due to the action of $-p(x, y)$ ($0 < x < vt,\ -\infty < y < \infty,\ z = \pm 0$) on the crack faces can be obtained by using the solution of Section 2. Following the arguments used by Freund (1990) for the mode I plane problem, the general expression of the stress intensity factor may be written as

$$K_{\mathrm{I}}(y, t) = \int_{-\infty}^{\infty} \int_{0}^{vt} k_{\mathrm{I}}^{\mathrm{F}}(y - y', t - x'/v) p(x', y')\, \mathrm{d}x'\, \mathrm{d}y', \tag{63}$$

which is useful for numerical computation when a general $p(x, y)$ is known.

In the next, particular tractions of constant distribution are considered. Firstly, we discuss the case of line load action. The traction can be expressed as

$$p(x, y) = -p_0 \delta(x), \quad -y_0 < y < y_0. \tag{64}$$

The stress intensity factor for this case is

$$K_{\mathrm{I}}(y, t) = p_0 \int_{-y_0}^{y_0} k_{\mathrm{I}}^{\mathrm{F}}(y - y', t)\, \mathrm{d}y'. \tag{65}$$

The Laplace transform of Eq. (65) is given by

$$\widehat{K}_{\mathrm{I}}(y, s) = p_0 \int_{-y_0}^{y_0} \widehat{k}_{\mathrm{I}}^{\mathrm{F}}(y - y', s)\, \mathrm{d}y'. \tag{66}$$

The substitution of (59) into the above equation leads to

$$\widehat{K}_{\mathrm{I}}(y, s) = \frac{p_0}{2\pi \mathrm{i}} \int_{\alpha_0 - \mathrm{i}\infty}^{\alpha_0 + \mathrm{i}\infty} \frac{1}{\xi} \bar{k}_{\mathrm{I}}^{\mathrm{F}}(\xi, s) \exp[s\xi(y + y_0)]\, \mathrm{d}\xi - \frac{p_0}{2\pi \mathrm{i}} \int_{\alpha_0 - \mathrm{i}\infty}^{\alpha_0 + \mathrm{i}\infty} \frac{1}{\xi} \bar{k}_{\mathrm{I}}^{\mathrm{F}}(\xi, s) \exp[s\xi(y - y_0)]\, \mathrm{d}\xi. \tag{67}$$

From Eq. (58) and in a similar fashion as Section 2.3, we obtain

$$K_{\mathrm{I}}(y,t)=\frac{\sqrt{2}p_0}{\pi^{3/2}}[J_1(|y|-y_0,t)-J_1(|y|+y_0,t)]\quad\text{for } |y|>y_0, \tag{68a}$$

$$K_{\mathrm{I}}(y,t)=\frac{\sqrt{2}p_0(1-c^2v^2)\sqrt{1+vp_1}}{(1+vc)S_+(v^{-1},0)\sqrt{\pi v(1-p_1^2v^2)}}t^{-1/2}-\frac{\sqrt{2}p_0}{\pi^{3/2}}[J_1(|y|-y_0,t)+J_1(|y|+y_0,t)]\quad\text{for } |y|<y_0, \tag{68b}$$

where

$$J_1(\lambda,t)=\frac{(1-c^2v^2)}{\sqrt{v(1-p_1^2v^2)}}\int_{a_0}^{t/\lambda}\mathrm{Im}\left\{\frac{\left[1+v\sqrt{p_1^2-(1-p_1^2v^2)\xi^2}\right]^{1/2}}{\xi\left[1+v\sqrt{c^2-(1-c^2v^2)\xi^2}\right]S_+(v^{-1},\xi)}\right\}\frac{\mathrm{d}\xi}{\sqrt{t-\lambda\xi}}. \tag{69}$$

Further, the solution for the traction of constant rectangular distribution can be obtained. In this case, the traction is expressed as

$$p(x,y)=-p_0,\quad 0<x<vt,\ -y_0<y<y_0. \tag{70}$$

The stress intensity factor for this case can be written as

$$K_{\mathrm{I}}^{\mathrm{p}}(y,t)=\int_0^{vt}K_{\mathrm{I}}(y,t-x'/v)\,\mathrm{d}x'. \tag{71}$$

Using Eqs. (68a) and (68b), we finally have

$$K_{\mathrm{I}}^{\mathrm{p}}(y,t)=\frac{2\sqrt{2}p_0}{\pi^{3/2}}[J_2(|y|-y_0,t)-J_2(|y|+y_0,t)]\quad\text{for } |y|>y_0, \tag{72a}$$

$$K_{\mathrm{I}}^{\mathrm{p}}(y,t)=\frac{2\sqrt{2}p_0v(1-c^2v^2)\sqrt{1+vp_1}}{(1+vc)S_+(v^{-1},0)\sqrt{\pi(1-p_1^2v^2)}}t^{1/2}-\frac{2\sqrt{2}p_0}{\pi^{3/2}}[J_2(|y|-y_0,t)+J_2(|y|+y_0,t)]\quad\text{for } |y|<y_0, \tag{72b}$$

where

$$J_2(\lambda,t)=\frac{v(1-c^2v^2)}{\sqrt{(1-p_1^2v^2)}}\int_{a_0}^{t/\lambda}\mathrm{Im}\left\{\frac{\left[1+v\sqrt{p_1^2-(1-p_1^2v^2)\xi^2}\right]^{1/2}}{\xi\left[1+v\sqrt{c^2-(1-c^2v^2)\xi^2}\right]S_+(v^{-1},\xi)}\right\}\sqrt{t-\lambda\xi}\,\mathrm{d}\xi. \tag{73}$$

4. Numerical results and discussions

The integrals in Eqs. (62) and (73) cannot be evaluated in terms of elementary functions. To make the physical meaning clear, a numerical integration of them is carried out for Poisson's material which is isotropic and for Beryl which is transversely isotropic.

Poisson's material: $a_1=a_2=3a_5$, $a_3=2a_5$, $a_4=a_5$, $c=1.088/\sqrt{a_5}$.
Beryl: $a_1=4.12484a_5$, $a_2=3.61802a_5$, $a_3=2.01199a_5$, $a_4=1.17363a_5$, $c=1.04645/\sqrt{a_5}$.

Numerical results for the fundamental solution are shown in Figs. 3 and 4 with the solid line representing Poisson's material and the dashed line representing Beryl. In the figures, the stress intensity factor history has been normalized by SIF $= k_{\mathrm{I}}^{\mathrm{F}}(y,t)(\pi y)^{3/2}$.

It is seen from the figures that upon the arrival of the dilatational wave, the initial response is dilatational and the crack faces tend to move towards each other, which is reflected by the stress intensity factor being negative. This phenomenon is intensified by the action of shear waves. When the Rayleigh wave arrives, the stress intensity factor becomes logarithmically singular. For Beryl, this process is delayed due to the material anisotropy. Thereafter, the crack faces begin to open and the stress intensity factor increases until it reaches a maximum. Then, the stress intensity factor decays gradually towards its limiting value of zero. It is seen that the presence of the anisotropy leads to the increase of the stress intensity factor.

It is observed that the stress intensity factor history is greatly affected by the extension speed of the crack. The faster the crack extends, the smaller the stress intensity factor becomes.

Figs. 5 and 6 display the variation of $J_2(\lambda,t)/\sqrt{\lambda}$ with normalized time. Unlike the fundamental solution, there is no singularity in the stress intensity factor when the Rayleigh wave arrives. It is also observed that the anisotropy leads to the increase of $J_2(\lambda,t)/\sqrt{\lambda}$.

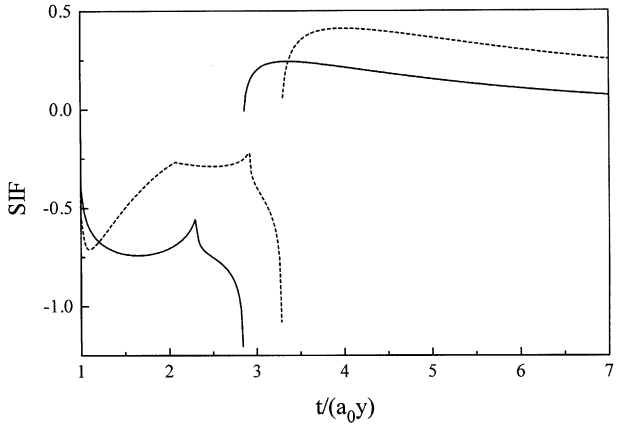

Fig. 3. The dynamic stress intensity factor history ($v = 0.8c_r$).

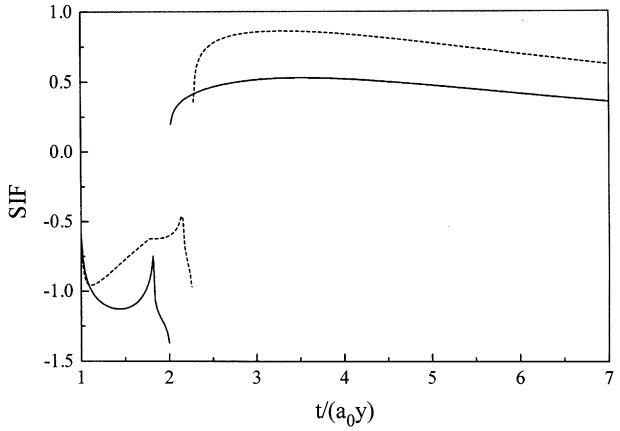

Fig. 4. The dynamic stress intensity factor history ($v = 0.4c_r$).

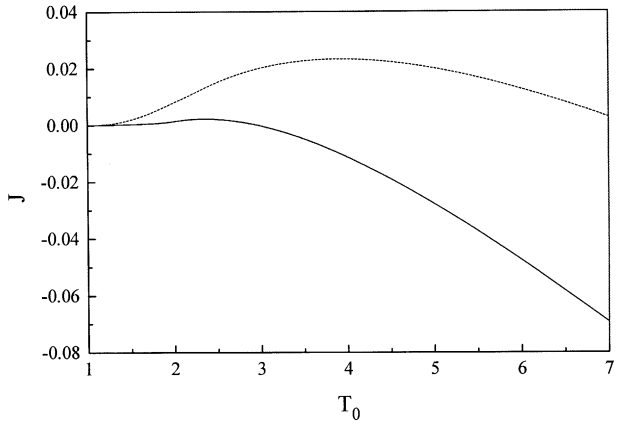

Fig. 5. The variation of J with normalized time T_0 ($J = J_2(\lambda, t)/\sqrt{\lambda}$, $T_0 = t/(a_0\lambda)$, $v = 0.8c_r$).

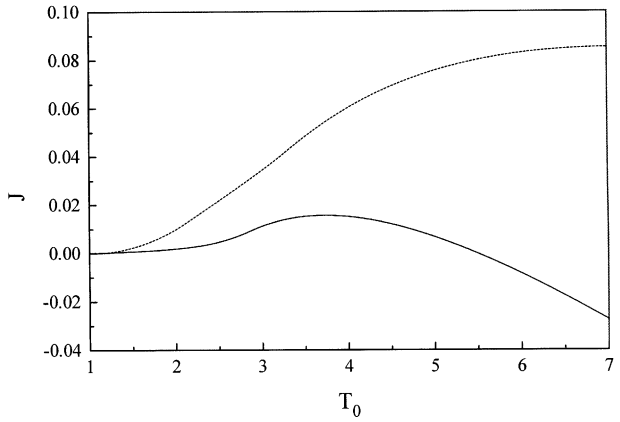

Fig. 6. The variation of J with normalized time T_0 ($J = J_2(\lambda, t)/\sqrt{\lambda}$, $T_0 = t/(a_0\lambda)$, $v = 0.4c_r$).

5. The conclusions

The mode I extension of a half plane crack in a transversely isotropic solid under 3-D loading is analyzed. Firstly, the fundamental problem that the crack is subjected to a pair of unit point loads on its faces is considered. The solution procedure is based on the use of transform methods, the Wiener–Hopf technique and the Cagniard–de Hoop method. An exact expression is derived for the mode I stress intensity factor as a function of time and position along the crack edge. Then, the stress intensity factor history due to general loading is obtained using the fundamental solution. Some features of the solutions are discussed through numerical results.

In the analysis, the half plane crack is assumed to propagate with a straight edge. For practical applications, this solution can be applied to the cases when loads are almost uniformly distributed in the y-direction. Under general loading, the crack edge may become curved during extension. However, the solution can also be applied when the edge curvature is large. For other cases, the curved edge may be treated as the perturbation of a straight line moving at a constant speed v and described as

$$x = vt + \varepsilon g_1(y, t) + \varepsilon^2 g_2(y, t) + \cdots, \tag{74}$$

where ε is a small parameter and $g_i(y,t)$ $(i=1,2,\ldots)$ are functions determined with an initiation criterion. From the above equation, we can see that the present solution serves as the zero order approximation of the problem. In order to obtain a complete solution, $g_i(y,t)$ $(i=1,2,\ldots)$ must be determined firstly with an initiation criterion. Unfortunately, this criterion has not yet been available for three-dimensional crack problems.

Acknowledgements

The financial support of this research by the Guangdong Provincial Natural Science Foundation and the Science Foundation of Shantou University is gratefully acknowledged.

References

Ang, W.T., 1988. A crack in an anisotropic layered material under the action of impact loading. J. Appl. Mech. 55, 120–125.
Ang, T., 1987. Transient response of a crack in an anisotropic strip. Acta Mech. 70, 97–109.
Dhawan, G.K., 1982a. Interaction of elastic waves by a Griffith crack in infinite transversely isotropic medium. Int. J. Fracture 19, 29–37.
Dhawan, G.K., 1982b. Interaction of SV-waves by a Griffith crack in infinite transversely isotropic medium. Int. J. Fracture 20, 103–110.
Freund, L.B., 1990. Dynamic Fracture Mechanics. Cambridge University Press, Cambridge.
Kassir, M.K., Bandyopadhyay, K.K., 1983. Impact response of a cracked orthotropic medium. J. Appl. Mech. 50, 630–636.
Kundu, T., Bostrom, A., 1991. Axisymmetric scattering of a plane longitudinal wave by a circular crack in a transversely isotropic solid. J. Appl. Mech. 58, 695–702.
Kundu, T., Bostrom, A., 1992. Elastic wave scattering by a circular crack in a transversely isotropic solid. Wave Motion 15, 285–300.
Kuo, A.Y., 1984a. Transient stress intensity factors of an interfacial crack between two dissimilar anisotropic half-spaces, Part 1. Orthotropic material. J. Appl. Mech. 51, 71–76.
Kuo, A.Y., 1984b. Transient stress intensity factors of an interfacial crack between two dissimilar anisotropic half-spaces, Part 2. Fully anisotropic material. J. Appl. Mech. 51, 780–786.
Lin, W., Keer, L.M., 1989. Three-dimensional analysis of cracks in layered transversely isotropic media. Proc. R. Soc. London A 424, 307–322.
Lobanov, E.V., Novichkov, Y.N., 1981. Diffraction of SH-waves by an oblique crack in an orthotropic half-space. Soviet Appl. Mech. 17, 610–615.
Mandal, S.C., Ghosh, M.L., 1994. Interaction of elastic waves with a periodic array of coplanar Griffith cracks in an orthotropic elastic medium. Int. J. Eng. Sci. 32, 167–178.
Mattsson, J., Niklasson, A.J., Eriksson, A., 1997. 3D ultrasonic crack detection in anisotropic materials. Res. Nondestr. Eval. 9, 59–79.
Norris, A.N., Achenbach, J.D., 1984. Elastic wave diffraction by a semi-infinite crack in a transversely isotropic material. Quart. J. Mech. Appl. Math. 37, 565–580.
Ohyoshi, T., 1973. Effect of orthotropy on singular stresses produced near a crack tip by incident SH-waves. ZAMM 53, 409–411.
Shindo, Y., Nozaki, H., Higaki, H., 1986. Impact response of a finite crack in an orthotropic strip. Acta Mech. 62, 87–104.
Shindo, Y., Higaki, H., Nozaki, H., 1992. Impact response of a single edge crack in an orthotropic strip. J. Appl. Mech. 59, s152–s157.
Tsai, Y.M., 1982. Penny-shaped crack in a transversely isotropic plate of finite thickness. Int. J. Fracture 20, 81–89.
Tsai, Y.M., 1988. Dynamic penny-shaped crack in a transversely isotropic material. Eng. Fract. Mech. 31, 977–984.
Zhang, C.H., 1992. Elastodynamic analysis of a periodic array of mode III crack in transversely isotropic solids. J. Appl. Mech. 59, 366–371.
Zhang, C.H., Gross, D., 1993. Interaction of antiplane cracks with elastic waves in transversely isotropic materials. Acta Mech. 101, 231–247.
Zhao, X., 2000. The impact response of a half plane crack in a transversely isotropic solid due to 3-D mixed mode loading. Int. J. Fracture 106, 357–371.
Zhao, X., 2001. The stress intensity factor history for a half plane crack in a transversely isotropic solid due to impact point loading on the crack faces. Int. J. Solids and Structures 38, 2851–2865.
Zhao, X., Xie, H., 1999. The 3-D stress intensity factor for a half plane crack in a transversely isotropic solid due to the motion of loads on the crack faces. Acta Mech. Sinica 15, 265–274.
Zhao, X., Xie, H., 2000. Elastodynamic analysis of a half plane crack in a transversely isotropic solid under 3-D transient loading. Acta Mech. 143, 35–45.